Measuring the Spectrum of Colored Noise by Dynamical Decoupling

Gonzalo A. Álvarez* and Dieter Suter†

Fakultät Physik, Technische Universität Dortmund, D-44221 Dortmund, Germany

(Received 12 June 2011; published 30 November 2011)

Decoherence is one of the most important obstacles that must be overcome in quantum information processing. It depends on the qubit-environment coupling strength, but also on the spectral composition of the noise generated by the environment. If the spectral density is known, fighting the effect of decoherence can be made more effective. Applying sequences of inversion pulses to the qubit system, we developed a method for dynamical decoupling noise spectroscopy. We generate effective filter functions that probe the environmental spectral density without requiring assumptions about its shape. Comparing different pulse sequences, we recover the complete spectral density function and distinguish different contributions to the overall decoherence.

DOI: 10.1103/PhysRevLett.107.230501 PACS numbers: 03.67.Pp, 03.65.Yz, 76.60.Es, 76.60.Lz

Introduction.—Quantum information processing relies on the robust control of quantum systems, which are always influenced by external degrees of freedom that disturb the quantum information by a process called decoherence [1]. Many strategies were developed to fight this degradation of information. These methods are based on error correction [2,3] or they decouple the environment [4–7]. Fighting decoherence successfully requires knowledge of the spectral distribution of the noise to design robust quantum processes [8–11].

One simple decoupling strategy is called dynamical decoupling (DD) [7,12]. It is based on the application of a sequence of control pulses to the system to effectively isolate it from the environment. Different DD sequences were developed [7,12–14] and tested experimentally [15–20]. If the pulses are ideal, the spectral density of the system-environment (SE) interaction becomes the dominant factor for the decoherence rate [8,14,15,19,21–26]. Consequently, a DD sequence has to be judiciously designed according to the particular noise spectral density to be decoupled [14,15,23–26]. The information obtained from the measurement of the noise spectral density can be very useful for developing a suitable error model and directing the search for an effective DD sequence [10,11,27,28].

In this Letter, we present a method to determine the spectral density of the SE interaction. The method is based on previous results that the decay rate of a qubit during DD is given by the overlap of the bath spectral density function and a filter function generated by the DD sequence [14,15,19,21–26]. The filter function is given by the Fourier transform of the SE interaction modified by the control pulses: each π pulse changes the sign of the SE coupling. When many DD cycles are applied to the system, the filter functions become a sum of δ functions [19] and the decoherence rate is given by a discrete sum of spectral densities. A judicious choice of the DD sequence thus allows one to probe the environmental spectral density at selected frequencies. Combining several measurements, it is possible to obtain a detailed picture of the noise spectral distribution. In the following, we describe an exact and simple method for obtaining general spectral density functions. This DD noise spectroscopy method extends recent approximate solutions that can be used only for specific cases [10,27].

A qubit as the noise probe.—We consider a single qubit $\hat{S}$ as the probe. It is coupled to the bath to be studied with a purely dephasing interaction. In a resonantly rotating frame of reference [6], the free evolution Hamiltonian is $\hat{\mathcal{H}}_f = \hat{\mathcal{H}}_{SE} + \hat{\mathcal{H}}_E$, where $\hat{\mathcal{H}}_E$ is the Hamiltonian of the environment and $\hat{\mathcal{H}}_{SE} = b_{SE}\hat{S}_z\hat{E}$ is a general pure dephasing interaction between system and environment. $\hat{E}$ is some operator of the environment and b_{SE} the SE coupling strength. This type of interaction is encountered in a wide range of solid-state spin systems, as, for example, nuclear spin systems in NMR [4,5,17,19], electron spins in diamonds [18], electron spins in quantum dots [29], donors in silicon [30], etc.

We consider the application of a sequence of short, strong pulses that invert the probe qubit [4,5,7,12]. We assume N instantaneous pulses at times t_i, with delays $\tau_i = t_i - t_{i-1}$ between the pulses for $i = 2, \ldots, N+1$ and $\tau_1 = t_1 - t_0$, where $t_0 = 0$ and $t_{N+1} = \tau_c$.

While such a sequence can refocus a static system-environment interaction completely, any time-dependence reduces its efficiency. We calculate the remaining decay rate for the case where the environment can be well described by stochastic noise. This is also valid for a quantum second order approximation of the time-dependent SE interaction [6]. We now eliminate the environment-Hamiltonian $\hat{\mathcal{H}}_E$ by using an interaction representation with respect to the evolution of the isolated environment. The system-environment Hamiltonian then becomes $\hat{\mathcal{H}}^{(E)}_{SE}(t) = b_{SE}\hat{S}_z e^{-i\hat{\mathcal{H}}_E t}\hat{E}e^{i\hat{\mathcal{H}}_E t}$. Since $\hat{\mathcal{H}}_E$ does not commute with $\hat{\mathcal{H}}_{SE}$, the effective system-environment

interaction $\hat{\mathcal{H}}_{SE}^{(E)}$ is time-dependent and the system experiences a fluctuating coupling with the environment. Tracing over the bath variables replaces $b_{SE}e^{-i\hat{\mathcal{H}}_E t}\hat{E}e^{i\hat{\mathcal{H}}_E t}$ by the stochastic function $b_{SE}E(t)$. For simplicity we assume that this random field has a Gaussian distribution with zero average, $\langle E(t)\rangle = 0$. The autocorrelation function is $\langle E(t)E(t+\tau)\rangle = g(\tau)$ and the spectral density $S(\omega)$ of the system-bath interaction is the Fourier transform of $b_{SE}^2 g(\tau)$.

The free evolution operator for a given realization of the random noise is $\exp\{-i\phi(t)\hat{S}_z\}$, where $\phi(t) = b_{SE}\int_0^t dt_1 E(t_1)$ is the phase accumulated by the probe spin during the evolution. Considering now the effect of the pulses, they generate reversals of $\hat{\mathcal{H}}_{SE}(t)$. If the pulses are applied during the interval τ_c as described above, the accumulated phase $\phi(M\tau_c)$ after M cycles becomes $\phi(M\tau_c) = b_{SE}\int_0^{M\tau_c} dt' f_N(t', M\tau_c)E(t')$, where the modulating function $f_N(\tau', M\tau_c)$ switches between ± 1 at the position of every pulse [23]. We set the initial state of the probe spin to $\hat{\rho}_0 = \hat{S}_{x,y}$ and calculate the evolution of the normalized magnetization under the effects of DD by taking the average over the random fluctuations: $\langle s_{x,y}(t)\rangle = e^{-(1/2)\langle\phi^2(t)\rangle}$. The resulting decay can be quantified by the exponential's argument

$$\tfrac{1}{2}\langle\phi^2(t)\rangle = R(t)t = \sqrt{\tfrac{\pi}{2}}\int_{-\infty}^{\infty} d\omega S(\omega)|F_N(\omega, M\tau_c)|^2, \quad (1)$$

where $F_N(\omega, M\tau_c)$ is the Fourier transform of $f_N(t', M\tau_c)$ [21–23]. The decay function $R(t)t$ is thus equal to the product of the spectral density $S(\omega)$ of the system-environment coupling and the filter transfer function $F_N(\omega, M\tau_c)$. We have recently shown that $F_N(\omega, M\tau_c)$ is a sum of sinc functions centered at the harmonic frequencies $k\omega_0 = 2\pi k/\tau_c$ of the Fourier series of $f_N(t', \infty)$ [19], which corresponds to the limit $M \to \infty$. Hence, for $t = M\tau_c \gg \tau_B$, the noise correlation time, the filter function $|F_N(\omega, \tau_M)|$ becomes an almost discrete spectrum given by the Fourier transform of $f_N(t', \infty)$; i.e., $F(\omega, t)$ becomes a series of δ functions centered at $k\omega_0$. Thus, in the limit of many cycles, the decay is exponential and $R(t)$ becomes time independent

$$R(t) = R = \sum_{k=1}^{\infty} A_k^2 S(k\omega_0), \quad (2)$$

with $A_k^2 = \frac{\sqrt{2\pi}}{\tau_c}|F_N(k\omega_0, \tau_c)|^2$, where for a CPMG sequence [4,5] with $\tau_2 = 2\tau_1 = 2\tau_3 = \tau$, $A_k \propto 1/k$ for odd k and 0 otherwise. This is the basis for the DD noise spectroscopy methodology presented in this Letter. Examples of the probe spin signal decay are shown in the inset of Fig. 1.

DD noise spectroscopy.—Assuming for the moment that the sum in Eq. (2) collapses to the $k = 1$ term, we can scan the bath spectral density by varying the delay between the pulses as in Refs. [10,27]. However, for real DD sequences, we always have an infinite series, where all harmonics contribute to the decay rate with the weight A_k. Determining the spectral density function therefore requires the inversion of Eq. (2) and thus the consideration of only the $k = 1$ term is a rough approximation. The main difficulty here is that a single measurement depends on an infinite number of unknown spectral density values. We solve this problem by a two-step procedure: in the first step, we combine m measurements with different pulse delays, which we choose such that they probe the spectral density function at a discrete set of harmonic frequencies with different sensitivity amplitudes A_k. In this step, we neglect contributions from the tail of $S(\omega > m\omega_{\min})$. This yields a square matrix that we can invert to obtain the values of $S(j\omega_{\min})$, $j = 1 \ldots m$. From the resulting spectral density function, we estimate a functional form for the tail of the distribution and correct the data for the contributions from the tail. Inverting the matrix again, with the corrected values, gives the final spectral density distribution.

A natural choice for the probing sequence is the CPMG or equidistant sequence, which has harmonics at frequencies $\omega_0 = \pi/\tau$. To simplify the inversion of Eq. (2), we choose the pulse delays in the different measurements such that all relevant frequencies, including all harmonics, are multiples of a minimal frequency $\omega_{\min}$. We therefore start with a maximum delay $\tau_{\max} = \pi/\omega_{\min}$, which determines the frequency resolution with which we probe the spectral density function. If the maximum frequency at which we want to probe the spectral density function directly is $m\omega_{\min}$, then we need to apply sequences with delays $\tau_n = \tau_{\max}/n = \tau_{\min}m/n$. If we neglect the contribution from frequencies $> m\omega_{\min}$, the relaxation rates R_n for the

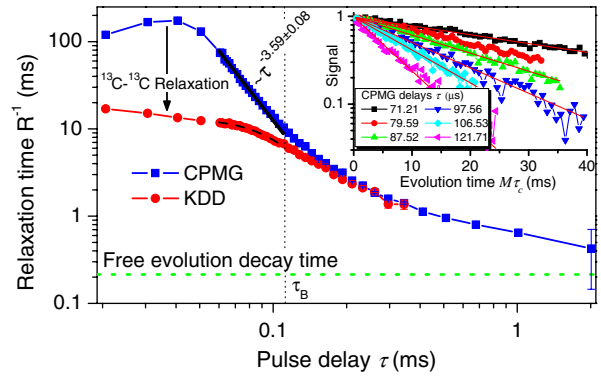

FIG. 1 (color online). Experimental relaxation times of the probe spin under the application of CPMG (squares) and KDD (circles) sequences. The black solid line represents a power law fitted to the CPMG data and the green dotted line the asymptotic free evolution decay rate. The black dashed line is a fit to the KDD data with an expression $(R_{^{13}C} + C'\tau^{\alpha})^{-1}$. Inset: Experimental signal decays of the probe spin as a function of the evolution time under CPMG dynamical decoupling. Different curves correspond to different pulse delays. The straight lines represent exponential fits.

different experiments are given by a system of m linear equations

$$R_n = \sum_{k=1}^{[m/n]} A_k^2 S(nk\omega_{\min}) = \sum_{j=1}^{m} U_{nj} S_j, \quad (3)$$

where $[m/n]$ denotes the integer part of m/n and $j = nk$. The elements A_k^2 form an upper triangular matrix $U_{nj} = \sum_{k=1}^{[m/n]} A_k^2 \delta_{j,nk}$, and $S_j = S(j\omega_{\min})$ represent the unknown spectral density values, which can formally be calculated as $S_j = \sum_{n=1}^{m} (U^{-1})_{jn} R_n$

We now correct for the omitted contributions from the high-frequency tail of the infinite sum by approximating it with a suitable functional form, which depends on the system being studied. Typical examples include a power law decay, Lorentzian or Gaussian decay, or a sudden cut off like in an Ohmic bath. In the system that we used as an example (see below), the experimental data can be approximated very well by a power law dependence, as shown in Fig. 1 (squares).

If the tail satisfies a power law $S_j = \frac{C}{j^\alpha}$ for $j > n_p$, then

$$R_{n>n_p} = \sum_{k=1}^{\infty} \frac{A_k^2 C}{(nk)^\alpha} = \frac{C}{n^\alpha} \sum_{k=1}^{\infty} \frac{A_k^2}{k^\alpha} = \frac{C\Lambda_\alpha}{n^\alpha}. \quad (4)$$

This relation is represented by the black solid line in Fig. 1. We can now modify Eq. (3) by adding the neglected terms and then the relaxation rates satisfy

$$R_n = \sum_{j=1}^{m} U_{nj} S_j + \left(\frac{\Lambda_\alpha C}{n^\alpha} - \sum_{j=1}^{m} U_{nj} \frac{C}{j^\alpha} \right), \quad (5)$$

where $(\frac{\Lambda_\alpha C}{n^\alpha} - \sum_{j=1}^{m} U_{nj} \frac{C}{j^\alpha}) = \frac{C}{n^\alpha} \sum_{k>m-n+1} \frac{A_k^2}{k^\alpha}$ represents the effective spectral density summing the contribution from all harmonics $k > m - n + 1$. The spectral density is now determined from $S_j = \sum_{n=1}^{m} (U^{-1})_{jn} (R_n - \frac{\Lambda_\alpha C}{n^\alpha}) + \frac{C}{j^\alpha}$. Equation (4) shows that for a power law dependence, the relaxation rate and the spectral density are proportional and thus for a qualitative description of $S(\omega)$ considering only the $k = 1$ term is enough validating the results of Refs. [10,27].

Experimental determination of $S(\omega)$.—For an experimental demonstration of this method, we chose ^{13}C nuclear spins ($S = 1/2$) as probe qubits. We used polycrystalline adamantane where the carbon nuclear spins are coupled to an environment of ^{1}H nuclear spins ($I = 1/2$) that act as a spin-bath. The natural abundance of the ^{13}C nuclei is about 1%, and to a good approximation each ^{13}C nuclear spin is surrounded by about 150 ^{1}H nuclear spins. The interaction with the environment is thus dominated by the ^{13}C-^{1}H magnetic dipole coupling [6]. To determine the bath spectral density we applied the equidistant sequences CPMG and KDD [20] to the probe spin for different delays between pulses $\tau_n = \tau_{\max}/n$, with $n = 1 \ldots 40$ and $\tau_{\max} = 2$ ms. Delays are measured between the center of the pulses. For CPMG, we chose an initial state longitudinal to the rf field of the refocusing pulses because then pulse error effects can be neglected [5,17]. The inset of Fig. 1 shows examples of the ^{13}C signal decays. The lines in the inset show the fitted exponential decays, which agree very well with the data points in this range. This demonstrates that we are in the regime where the filter functions are discrete. KDD was shown to be robust against pulse errors, independent of the initial condition (see Ref. [20] for details). For ideal pulses, both sequences have the same filter function. As shown in Fig. 1 (squares) the observed relaxation times for this system depend on the pulse spacing like $\propto \tau^{-3.59}$ for the CPMG sequence over the range $\tau = [50\ \mu\text{s}, 110\ \mu\text{s}]$. We only used the data points for $\tau > 50\ \mu$s to determine the parameters C and α, since Fig. 1 indicates that other processes contribute to the relaxation at shorter delays. From the fitting process, we found $\alpha = 3.59 \pm 0.08$ and $\Lambda_\alpha \approx 1.002$. Here, the contribution of the infinite series of 2×10^{-3} is almost negligible. Figure 1 also shows that the dependence of the decoherence rates changes at $\tau \gtrsim 100\ \mu$s. This agrees with the value that we determined earlier for the correlation time of the bath τ_B [17] in adamantane.

If KDD is used for decoupling, we observe that the relaxation time saturates for τ shorter than 50 μs and in general is shorter than for CPMG (Fig. 1, circles). This difference can be attributed to the effect of ^{13}C-^{13}C couplings. Because in the CPMG sequence all pulses generate the same rotation, the overall effect of the pulse cycle is to first order equivalent to a constant effective field, which stabilizes the observable magnetization against the effect of ^{13}C-^{13}C couplings [31]. In the KDD case, the state is not longitudinal to the pulses and no spin-lock effect is observed. The saturation of the relaxation time for the CPMG case for $\tau < 50\ \mu$s can be attributed to the finite rf field strength or, equivalently, to the finite duration of the pulses. Pulse errors may also contribute in this regime.

In the KDD case, the ^{13}C-^{13}C interaction dominates over the effect of the proton bath for short pulse delays. To verify this, we assumed a ^{13}C-^{13}C relaxation rate $R_{^{13}\text{C}}$ independent of the pulse delays and fitted the expression $(R_{^{13}\text{C}} + C'\tau^\alpha)^{-1}$ over the range [50 μs, 110 μs] where the CPMG data follow a power law (dashed line in Fig. 1). We obtained $R_{^{13}\text{C}} = (75 \pm 1)\ \text{s}^{-1}$ and $\alpha = 3.7 \pm 0.3$, which perfectly matches with the CPMG result. If we subtract the $R_{^{13}\text{C}}$ contribution, we obtain the spectral density represented by the empty circles in Fig. 2, which are almost identical to the result obtained with the CPMG sequence (solid squares).

We demonstrate with Eq. (4) that the qualitative behavior of the power law tail can be well obtained by the first harmonic approximation ($k = 1$) that is proportional to the exact solution derived from (5). For lower frequencies, the corrections from our exact method can be relevant (squares vs rombuses in Fig. 2). However, because $S(\omega)$ decays rapidly, the difference is small in this case.

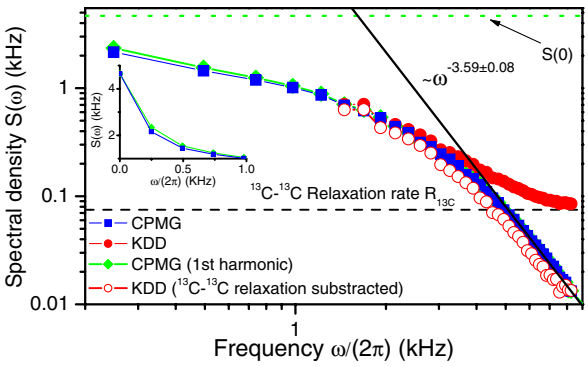

FIG. 2 (color online). Experimentally determined noise spectral density. The inset shows in a linear scale the low frequency regime. The green dotted line represents the free evolution decay rate of the probe spin, i.e., $S(0)$.

This is not always true, as we now show with a specific example: We modulate the system-environment interaction by applying a resonant radio-frequency field to the proton spins, which periodically inverts them. Using the same measurement procedure, we obtained the data shown in Fig. 3.

The approximate solution $S(n\omega_{\min}) = R_n/A_1^2$, where only the first harmonic ($k = 1$) is considered, shows a main peak at the modulation frequency Ω and some satellite peaks at at lower frequencies that are integer fractions of Ω. These satellite peaks are artefacts of the data analysis that neglects contributions from higher harmonics of the filter function of Eq. (2). Using our method, we obtain an improved solution where the satellite peaks are eliminated. The spectral density distribution for this case is qualitatively different from that of the unmodulated case. In particular, the value at zero frequency is reduced, but a maximum has appeared at the modulation frequency. This has important consequences for implementing dynamical

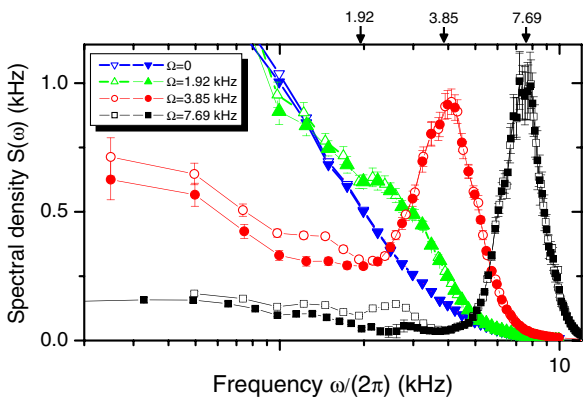

FIG. 3 (color online). Experimentally determined noise spectral density for a modulated system-environment interaction. The empty symbols were obtained when only the first harmonic was considered, the full symbols show the results from the exact method.

decoupling: For $\Omega = 7.69$ kHz, good decoupling performance is expected for $\tau \sim 0.12$ ms, where the first harmonic is at the spectral density minimum near 4 kHz. Increasing the decoupling rate then would drastically reduce the decoupling performance, in stark contrast to the usual expectation that it should increase with the decoupling rate.

Conclusions.—We have developed a method to determine the noise spectral density generated by a bath. It is based on modulating the system-environment interaction by applying sequences of inversion pulses to the system. If the sequence consists of many repetitions of a basic cycle, the resulting decays are exponentials and the decay rates are given by the spectral density at discrete frequencies. This allows one to build a linear system of equations that can be inverted to obtain the unknown spectral density function. We applied the method to obtain the spectral density of the ^{13}C-^{1}H interaction in adamantane. Applying this method to other systems will help fighting decoherence, e.g., by optimizing DD sequences by reducing the overlap of their filter functions with the noise spectral density [14,15,23–26]. In particular, in the natural spin-boson model where the spectral density grows with the frequency until a cut off, our high order method becomes important. Moreover, many naturally occurring systems, also contain discrete features in the noise spectrum, such as the Larmor precession of the ^{13}C nuclei, which are the dominant source of decoherence for the electrons of the diamond NV center [18]. In this case, neglecting the higher harmonics leads to erroneous additional resonances. Our method also complements standard NMR techniques that use CPMG sequences to distinguish between different sources of inhomogenities [32] or measuring diffusion rates [33–35] as well as protein dynamics rates [36] in liquid state NMR. Those methods determine correlation times but assume specific spectral density functions, while our technique is suitable for the determination of spectral densities with unknown shape.

This work is supported by the DFG through Su 192/24-1. G. A. A. is thankful for financial support from the Alexander von Humboldt Foundation in the initial stage of this project. We thank Alexandre M. Souza for helpful discussions.

Note added in proof.—A similar work was recently published [37].

*gonzalo.alvarez@tu-dortmund.de
†Dieter.Suter@tu-dortmund.de

[1] W. H. Zurek, Rev. Mod. Phys. **75**, 715 (2003).
[2] J. Preskill, Proc. R. Soc. A **454**, 385 (1998).
[3] E. Knill, Nature (London) **434**, 39 (2005).
[4] H. Y. Carr and E. M. Purcell, Phys. Rev. **94**, 630 (1954).
[5] S. Meiboom and D. Gill, Rev. Sci. Instrum. **29**, 688 (1958).

[6] A. Abragam, *Principles of Nuclear Magnetism* (Oxford University Press, London, 1961).
[7] L. Viola, E. Knill, and S. Lloyd, Phys. Rev. Lett. **82**, 2417 (1999).
[8] J. Zhang, X. Peng, N. Rajendran, and D. Suter, Phys. Rev. A **75**, 042314 (2007).
[9] D. D. Bhaktavatsala Rao and G. Kurizki, Phys. Rev. A **83**, 032105 (2011).
[10] J. Bylander, S. Gustavsson, F. Yan, F. Yoshihara, K. Harrabi, G. Fitch, D. G. Cory, Y. Nakamura, J. Tsai, and W. D. Oliver, Nature Phys. **7**, 565 (2011).
[11] I. Almog, Y. Sagi, G. Gordon, G. Bensky, G. Kurizki, and N. Davidson, J. Phys. B **44**, 154006 (2011).
[12] W. Yang, Z. Wang, and R. Liu, Front. Phys. **6**, 2 (2010).
[13] K. Khodjasteh and D. A. Lidar, Phys. Rev. Lett. **95**, 180501 (2005).
[14] G. S. Uhrig, New J. Phys. **10**, 083024 (2008).
[15] M. J. Biercuk *et al.*, Nature (London) **458**, 996 (2009).
[16] J. Du *et al.*, Nature (London) **461**, 1265 (2009).
[17] G. A. Álvarez, A. Ajoy, X. Peng, and D. Suter, Phys. Rev. A **82**, 042306 (2010).
[18] C. A. Ryan, J. S. Hodges, and D. G. Cory, Phys. Rev. Lett. **105**, 200402 (2010).
[19] A. Ajoy, G. A. Álvarez, and D. Suter, Phys. Rev. A **83**, 032303 (2011).
[20] A. M. Souza, G. A. Álvarez, and D. Suter, Phys. Rev. Lett. **106**, 240501 (2011).
[21] A. G. Kofman and G. Kurizki, Phys. Rev. Lett. **87**, 270405 (2001).
[22] A. G. Kofman and G. Kurizki, Phys. Rev. Lett. **93**, 130406 (2004).
[23] L. Cywinski, R. M. Lutchyn, C. P. Nave, and S. DasSarma, Phys. Rev. B **77**, 174509 (2008).
[24] G. Gordon, G. Kurizki, and D. A. Lidar, Phys. Rev. Lett. **101**, 010403 (2008).
[25] H. Uys, M. J. Biercuk, and J. J. Bollinger, Phys. Rev. Lett. **103**, 040501 (2009).
[26] J. Clausen, G. Bensky, and G. Kurizki, Phys. Rev. Lett. **104**, 040401 (2010).
[27] C. A. Meriles, L. Jiang, G. Goldstein, J. S. Hodges, J. Maze, M. D. Lukin, and P. Cappellaro, J. Chem. Phys. **133**, 124105 (2010).
[28] K. C. Young and K. B. Whaley, arXiv:1102.5115.
[29] R. Hanson *et al.*, Rev. Mod. Phys. **79**, 1217 (2007).
[30] B. E. Kane, Nature (London) **393**, 133 (1998).
[31] G. E. Santyr, R. M. Henkelman, and M. J. Bronskill, J. Magn. Reson. **79**, 28 (1988).
[32] A. N. Garroway, J. Magn. Reson. **28**, 365 (1977).
[33] E. O. Stejskal, J. Chem. Phys. **43**, 3597 (1965).
[34] E. O. Stejskal and J. E. Tanner, J. Chem. Phys. **42**, 288 (1965).
[35] K. J. Packer, J. Magn. Reson. **9**, 438 (1973).
[36] A. Mittermaier and L. E. Kay, Science **312**, 224 (2006).
[37] T. Yuge, S. Sasaki, and Y. Hirayama, Phys. Rev. Lett. **107**, 170504 (2011).